Report on JINR activities and tasks accomplished in 2010 in the frame of agreement about "Joint Underground Laboratory in Europe" "LEA-JOULE"

Dubna, 2011

January 2011

Report on JINR activities and tasks accomplished in 2010 in frame of agreement about "Joint Underground Laboratory in Europe" ("LEA-JOULE")

This document prepared on behalf of JINR LSM users by O. Kochetov and E. Yakushev [1]

The JOULE agreement has been signed between JINR and LSM (represented by CNRS and CEA) on 24 October 2005. The agreement reflects long historical participation of JINR scientists at different research activities conducting at LSM. With regards of highly fruitful cooperation between JINR and LSM in time of 2005-2008 years thanks to the agreement, in beginning of 2009 it has been extended for 4 more years with new participants 1) Russian Foundation for Basic Research and 2) Czech Technical University in Prague.

LEA-JOULE activity in LSM is linked with all experiments conducted in it. In particular with:

NEMO3 dedicated to double beta decay investigation and search of 0ν2β decay;

Super-NEMO further development of 0ν2β decay search on an unprecedented level of sensitivity;

EDELWEISS2 dedicated to direct search for non-baryonic dark matter;

TGV dedicated to search for double beta decay processes ($\beta^+\beta^+$, β^+EC, EC/EC) of ^{106}Cd;

SHIN dedicated to search for the presence of super heavy elements in nature.

Also, in a frame of the JOULE program, JINR group continue study of background environment of LSM, in particular neutron flux measurements and measurements of radon activity with a high sensitive radon monitor developed and built by JINR. In 2010 this program has been further extended with development of new radiochemical methods for detection of ultra low radioactivity of samples using in investigation of rare processes as well for development of methods of purification. As part of this activity ultra high sensitive germanium detector has been delivered to the LSM by JINR and CTU. Another detector available at LSM has been repaired and commissioned for low background investigations.

Reports about particular activities of JINR group at LSM are given below.

[1] Corresponding author: yakushev@jinr.ru

EDELWEISS2

The EDELWEISS experiment is dedicated to the search for non-baryonic cold dark matter in the form of WIMPs. The direct detection principle consists in measurement of the energy released by nuclear recoils produced in an ordinary matter target by elastic collisions of WIMPs from Milky Way galaxy. The EDELWEISS detectors are cryogenic (work temperature is 18 mK) Ge bolometers with simultaneous measurement of phonon and ionization signals. The comparison of the two signals provides a highly efficient event-by-event discrimination between nuclear recoils (induced by WIMP and also by neutron scattering) and electrons. A long-standing issue with these detectors is the reduction of the charge collection efficiency for interactions occurring close to their surface, which can impair significantly the discrimination between nuclear and electron recoils. This problem has been resolved by building of Ge/NTD/INTERDIGIT detectors using coplanar grid electrodes for event localization. In 2010, the EDELWEISS collaboration continued worked in 2 main directions: accumulation of statistic with already build bolometers and testing and calibration of newly installed detectors which allowed active rejection of surface background. New 800g FID detectors with significantly increased fiducial volume were start to be tested for its applicability in EDELWEISS and for it potential in reduction of the surface background.

The EDELWEISS experiment required unprecedented level of background understanding. In collaboration we target it study from both sides: experimental and modelling. In EDELWEISS the 2 important sources of background: neutrons and radon are under continuous control. Monitoring of neutron field at LSM is going on with 2 high sensitive low background neutron detection systems developed by JINR group. Continuous measurements of neutrons in LSM last from 2006. Now both fast and thermal neutron fluxes are under control. Mobility of the thermal neutron detector was allowed to conduct measurements at different places at LSM, and even inside of EDELWEISS's shields. Level of the detector's sensitivity on an order of 10^{-9} n/cm^2/sec was applied for direct test of efficiency of EDELWEISS-II shields to ambient neutron background. This measurement is extremely important from point of view WIMP background free experiment. Measurements at different locations at LSM further improving and make broaden our knowledge about neutron flux and it changes in the underground laboratory. Another dangerous source of background is radon. Radon is a noble gas which due it mobility and radioactivity of its daughters is extremely dangerous for EDELWEISS experiment. With build by JINR group high sensitive radon detection system now the radon level at environment of the EDELWEISS' cryostat is under continuous control during WIMP data taking. This is a key for unbiased interpretation of WIMP results at EDELWEISS. Modeling of background is also important part of work at EDELWEISS collaboration. This is one of the point of JINR-IN2P3 collaboration. One of the main detected backgrounds is coming from trace contamination of surface of detectors with radon daughters. For proper understanding of experimental data (location of contamination, for example), MC of background is needed. The main problem is arising because it is necessarily to model low energy region (from few keV). We continue work in this direction, from making the particle generators of decay of radon daughters to performing extensive simulations with low energy physics packages in GEANT4 and Penelope.

A total effective exposure of 322 kg day for WIMP search has been obtained after 1 year of EDELWEISS-II operation in 2009-2010 with using Ge/NTD/INTERDIGIT detectors. The observation of few nuclear recoil candidates above 20 keV was interpreted in terms of limits on the cross-section of spin independent interactions of WIMPs and nucleons. Cross-sections of 5.0×10^{-44} cm^2 are excluded at 90% CL for WIMP masses of 80 GeV/c^2. This is one of 3 best results on the moment (together with CDMS and XENON100 experiments). Further analysis are going on in order to reduce the effective threshold of the detectors to better address the case of lower-mass WIMPs. The EDELWEISS Collaboration aims to increase the

cumulated mass of the detectors in operation at the LSM, in order to soon probe the physically significant 10^{-44} cm^2 range of spin-independent WIMP-nucleon cross-section and be able to achieve sensitivity to an important class of SUSY ("Focus Point") models.

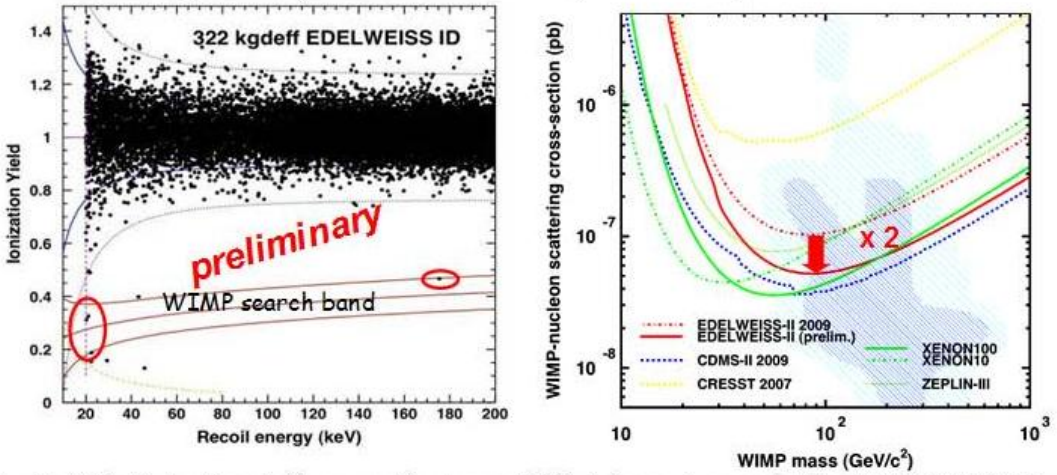

Fig. 1: *Left: Ionization yield vs recoil energy of fiducial events recorded by EDELWEISS-II in an exposure of 322 kg.d. The WIMP search region is defined by recoil energies greater than 20 keV (vertical dashed line). The 90% acceptance nuclear and electron recoil bands (full blue and red lines, respectively) are calculated using the average detector resolutions. Also shown as dashed lines are the 99.98% acceptance band and the 3 keV ionization threshold. Right: Limits on the cross-section for spin-independent scattering of WIMPs on nucleons as a function of WIMP mass from EDELWEISS-II year 2010 data together with limits from other direct WIMP searches.*

The scientific program for the future 12 months:

At EDELWEISS-II experiment next years low backgrounds physics runs will be continued with the aim to reach sensitivity to WIMP-nucleon SI cross-section of 10^{-44} cm^2 or better for a WIMP with mass of 100 GeV. Additional detectors of Ge/NTD/INTERDIGIT type and new 800g FID detectors with significantly increased fiducial volume will be added in the two coming years to experiment to enhance progressively the sensitivity to WIMPs. The aim is to have in next 2 years 3500 kg.d with no surface background events at nuclear recoil band above 15 keV threshold. This will provide the sensitivity on the 4×10^{-45} cm^2 level in successful competition with other world leading dark matter search experiments (Xe, Ar based, and CDMS).

Dubna team participates and makes commitment to follow parts of EDELWEISS-II project: 1) Assembly and commissioning of EDELWEISS-II; 2) Data taking (include daily routine procedures, as well as regular and special calibration runs); 3) Low background study and development of methods of neutron and radon detection; 4) Detector simulations and data analysis. Both participation in joint MC developments and participation in controlling of experiment (stability of data taking, calibration, etc).

Recent results received in our collaboration have been published at:

E. Armengaud et al. (EDELWEISS collaboration), "First results of the EDELWEISS-II WIMP search using Ge cryogenic detectors with interleaved electrodes", Physics Letters B 687 (2010), 294-298

A. Broniatowski et al. (EDELWEISS collaboration), "A new high-background-rejection dark matter Ge cryogenic detector", Physics Letters B, B 681 (2009), 305-309

V. Kozlov et al. (EDELWEISS collaboration), "A detection system to measure muon-induced neutrons for direct Dark Matter searches", Astropart. Phys. 34 (2010) 97-105

NEMO3

The objective of the NEMO 3 experiment is to search for the double beta decay process with two ($2\nu\beta\beta$ decay) or zero ($0\nu\beta\beta$ decay) neutrinos in the final state in the seven different $\beta\beta$ isotopes listed in the Table 1 with total weight at almost 10 kg. The experimental search for $0\nu\beta\beta$ decay is of major importance in particle physics. If this process is observed then it will reveal the Majorana nature of the neutrino ($\nu \equiv \overline{\nu}$) and may allow an access to the absolute neutrino mass scale. The process $0\nu\beta\beta$ decay violates the principle of lepton number conservation and is, therefore, a direct probe for physics beyond the Standard Model. The $2\nu\beta\beta$ decay process is a rare second order weak interaction process. The accurate measurement of its rate of decay is important since it constitutes the ultimate background in the search for $0\nu\beta\beta$ decay signal and is a valuable input for the theoretical calculations of the nuclear matrix elements.

Table 1. *Double beta decay isotopes studied at NEMO3*

Isotope	Mass (g)	$Q_{\beta\beta}$ (keV)	S/B
^{100}Mo	6914	3034	40
^{82}Se	932	2995	4
^{116}Cd	405	2805	7.5
^{150}Nd	37.0	3367	2.8
^{96}Zr	9.4	3350	1.
^{48}Ca	7.0	4272	6.8
^{130}Te	454	2529	0.25

The goals of the NEMO-3/SuperNEMO projects are to reach 0.2-1.0/0.04-0.1 eV sensitivities for the effective Majorana neutrino mass $\langle m_\nu \rangle$ ($T_{1/2}^{0\nu\beta\beta}$ (^{100}Mo) ~ $4 \cdot 10^{24}$/ $T_{1/2}^{0\nu\beta\beta}$ (^{82}Se) ~ $2 \cdot 10^{26}$ y) respectively.

In the year 2010 the NEMO-3 detector is completing the data taking. The total NEMO-3 statistics accumulated since February 2003 till November 2010 is ~ 2246 days (6.1 years). The updated results of the $2\nu\beta\beta$-decay search based on the use of 4.5 years of data have been presented at conferences in 2010: $T_{1/2}^{0\nu\beta\beta}(^{100}\text{Mo}) > 10^{24}$ y, $\langle m_\nu \rangle < 0.47$ - 0.96 eV (90%C.L.). The studies of $2\nu\beta\beta$-mode have been continued. The result of the ^{96}Zr half-life measurement is $T_{1/2}(^{96}\text{Zr}) = [2.35 \pm 0.14(\text{stat.}) \pm 0.16(\text{syst.})] \times 10^{19}$ y (see Fig. 2).

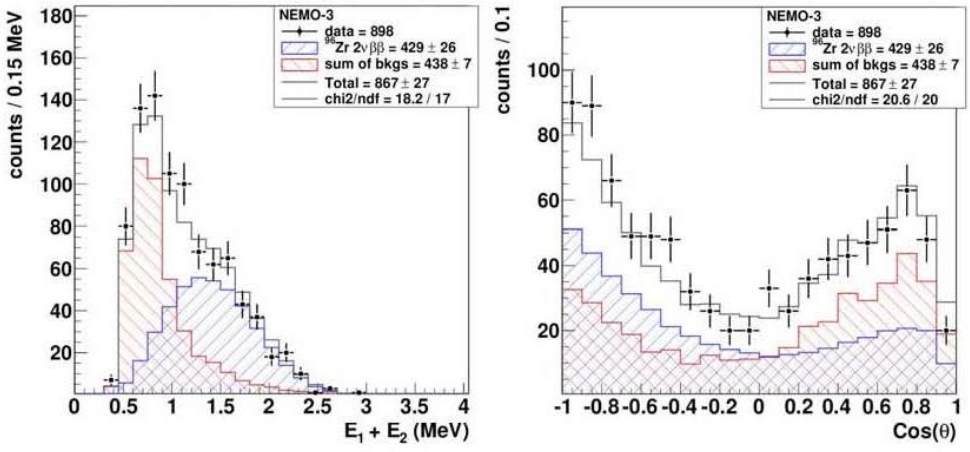

Fig. 2: *The distributions of total electron energy (left) and angle between electrons (right) in ^{96}Zr $2\nu\beta\beta$-process measured by the NEMO-3 detector.*

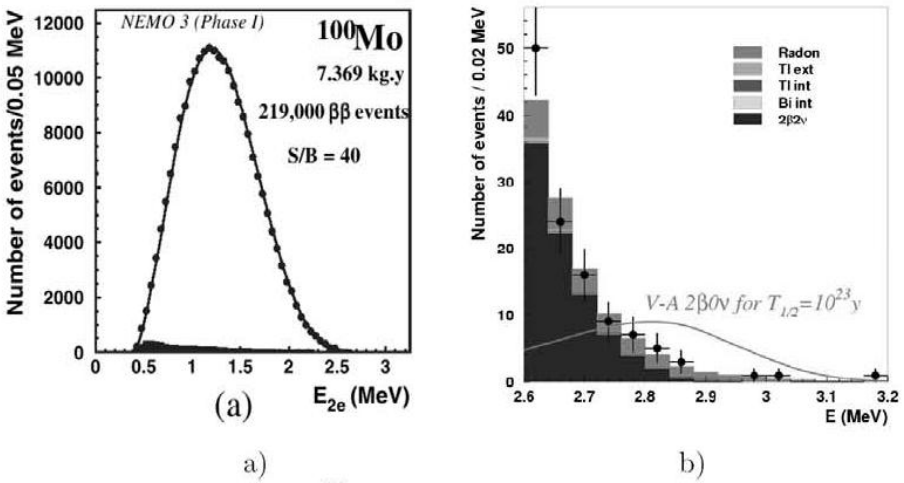

Fig. 3: *a) The energy sum spectrum of ^{100}Mo $\beta\beta_{2\nu}$ events with background subtracted (shown in black). b) The energy sum spectrum of two-electron events in ^{100}Mo at $Q_{\beta\beta}$.*

The experimental spectrum for main isotope studied at NEMO3 (^{100}Mo) is demonstrated on the Fig. 3.a. For this isotope the world largest dataset (219000 double beta events) with a signal to background ratio (S/B) of 40 has been accumulated. This provided precision determination of half-life of the double beta decay isotope, which was obtained to be $T_{1/2}^{2\nu}(^{100}Mo) = 7.11 \pm 0.02^{stat} \pm 0.54^{syst} \times 10^{18}\, y$. Measurements of the 2νββ were performed for 7 isotopes available in NEMO-3. Results are presented in Table 2.

Table 2: *NEMO-3 results of measurements of the 2νββ-decay half-lives.*

Isotope	Mass (g)	$Q_{\beta\beta}$ (keV)	Signal/Background	$T_{1/2}$ [10^{19} years]
^{100}Mo	6914	3034	40	0.711 ± 0.002 (stat) ± 0.054 (syst)
^{82}Se	932	2995	4	9.6 ± 0.3 (stat) ± 1.0 (syst)
^{116}Cd	405	2805	7.5	2.8 ± 0.1 (stat) ± 0.30 (syst)
^{150}Nd	37.0	3367	2.8	0.920 ± 0.025 ± 0.073 (syst)
^{96}Zr	9.4	3350	1.0	2.35 ± 0.14 (stat) ± 0.19 (syst)
^{48}Ca	7.0	4772	0.8	4.4 ± 0.5 (stat) ± 0.4 (syst)
^{130}Te	454	2529	0.25	69 ± 9 (stat) ± 10 (syst)

From all accumulated data no evidence for ββ0ν signal was found (Fig.3.b). A preliminary counting analysis shows 14 events in the window of interest [2.78–3.20] MeV, with expected background of 13.4. The analysis of the data taken is shown no signal observed in the molybdenum and selenium. The limits on the $T_{1/2}^{0\nu}$ and the corresponding $\langle m_\nu \rangle$ limits calculated using the recent NME values are:

$T_{1/2}^{0\nu}(^{100}\text{Mo}) > 5.8 \cdot 10^{23}$ y (90% C.L.) $\quad \langle m_\nu \rangle < 0.61 - 1.26$ eV

$T_{1/2}^{0\nu}(^{82}\text{Se}) > 2.1 \cdot 10^{23}$ y (90% C.L.) $\quad \langle m_\nu \rangle < 1.4 - 2.2.$ eV

Stable data taking with NEMO-3 detector requires continuous careful survey and maintenance of the apparatus especially with taking into account aging effects. Energy and time calibrations with radioactive sources performed on a regular biweekly base, laser calibration data is taken every day. For above purposes, physicists have to take shifts at the LSM. The Dubna group takes essential part in all these operations. In general main JINR contributions to the projects are: NEMO-3 running, calibrations, data analysis.

The NEMO3 program for the future 12 months is connected with started disassembly the experimental setup. JINR group will take significant part in this work. Scientific program for 2011 include final analysis of the total accumulated statistics with NEMO-3.

Main publications in 2010: J.Argyriades et al., Nucl. Phys. A 847 (2010) 168-179; Argyriades et al., Nucl. Instr. Met. A 622 (2010) 120-128. ; J.Argyriades et al., Nucl. Instr. Met. A 625 (2011) 20-28. ; R.Arnold et al., Eur. Phys. J. C 70 (2010) 927-943.

SuperNEMO R&D

SuperNEMO project is logical continuation of the NEMO3 project with increased mass of double beta decay sources, improved performance of the detector and with unprecedented level of background. In 2010 the SuperNEMO R&D program has been focused on the construction of the SuperNEMO Demonstrator (first module, see Fig.4). The main efforts have been concentrated on mechanical design based on a modules (tracker, calorimeter, and source frame) built separately, calorimeter studies (final choice of optimal parameters for calorimeter channels), electronics R&D, simulation, calibration and monitoring studies, source enrichment and purification. Results of the BiPo-1 prototype for radio purity measurements for the SuperNEMO double beta decay source foils have been published. Feasibility of reaching the required sensitivity of A(^{208}Tl) < 2 μBq/kg is demonstrated and construction of the BiPo-3 detector (see Fig.5) aimed to control radiopurity of source foils for the Demonstrator has been started.

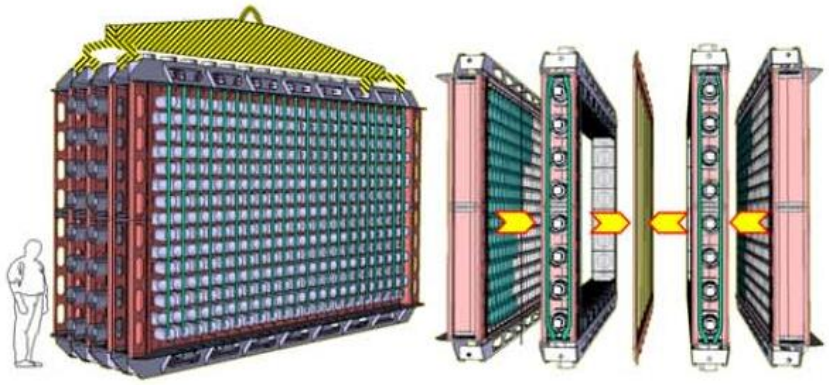

Fig 4: *The design of the SuperNEMO demonstrator (first module).*

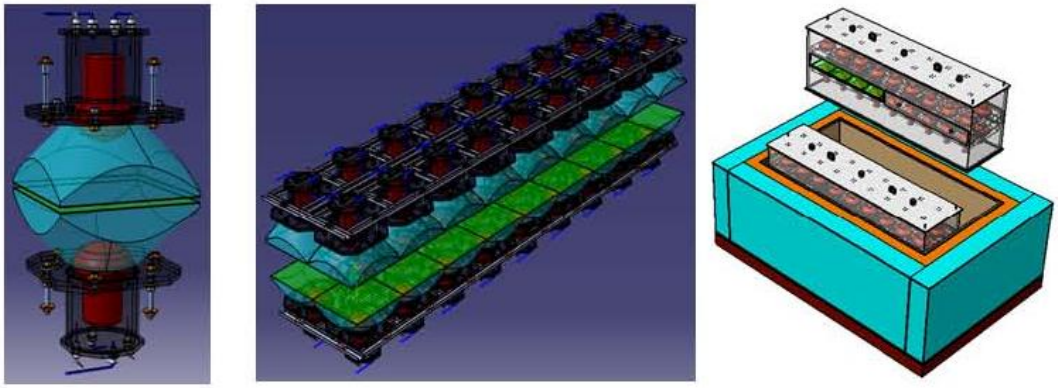

Fig 5: *The BiPo-3 capsule (on the left), module (in the middle), and the whole setup (on the right).*

An important R&D performed at LSM by JINR group is connected with energy monitoring and calibration of a calorimeter using alpha sources. Energy calibration and reliable long-term energy calibration stability control are subjects of crucial importance for calorimeters in modern large-scale setups (such as HEP or low background experiments) due to their long life cycle (many years). While energy calibration is carried out with radioactive sources, test beams, and background channels, monitoring is usually performed by a light survey system based on light-emitting diodes (LEDs) or lasers. Reliable control of stability is quite a challenging task, which leads to unavoidable complexity and cost in a light survey system constructed under a "one light - multiple modules" principle. On the other hand "one light -

one module" techniques might also be considered, e.g. each module could be equipped with a relatively cheap LED. The main problem of this approach is the difficulty in maintaining proper control of variations in the light injected by multiple sources. For large scale calorimeters an intermediate approach can be adopted: several light sources, each feeding a number of calorimeter modules. Use of quasi-monochromatic, long-lived alpha sources for energy calibration and monitoring of a calorimeter has great potential. A list of alpha-radioactive nuclei most suitable for calibration and monitoring purposes is given in Table 3. The gadolinium isotope is the best choice as it is a mono energetic α-source without any other decay channels. The other isotopes emit X-rays, electrons or γ-rays with energies up to the 1 MeV scale, which could be problematic for some low back round experiments. Despite low branching ratios such electrons and γ-rays might be detected in long-term exposure and even mimic the rare signal being sought.

Table 3: *Long-lived alpha sources, which can be used for calibration and monitoring.*

Isotope	Decay half-life, y	Main α-s: Energy, MeV (intensity, %)	Other decay modes
^{148}Gd	74.6	3.183 (100)	None
^{242}Pu	3.76×10^5	4.90 (76), 4.86 (23)	β^-, γ-s
^{240}Pu	6.5×10^3	5.17 (73), 5.12 (27)	β^-, γ-s
^{238}Pu	87.7	5.50 (71), 5.46 (29)	β^-,γ-s
^{241}Am	432.7	5.49 (85), 5.44 (15)	β^-, γ-s

We used ^{148}Gd obtained by irradiating of erbium with 0.6 GeV protons from the JINR synchrophasotron (Dubna, Russia). Three different techniques were developed to prepare sources which could be used for calibration and monitoring. First method is implantation of radioactive atoms by electromagnetic mass separator (EMS). Second method is sorption (planting) of low-soluble compounds containing an α-source on the surface of a scintillator (Fig. 6).

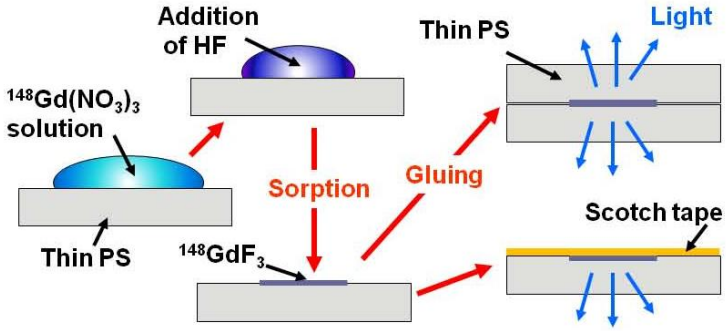

Fig. 6: *Technique to prepare light sources by sorption.*

The third technique is so called Light alpha sources. LS design is shown in Fig. 7.

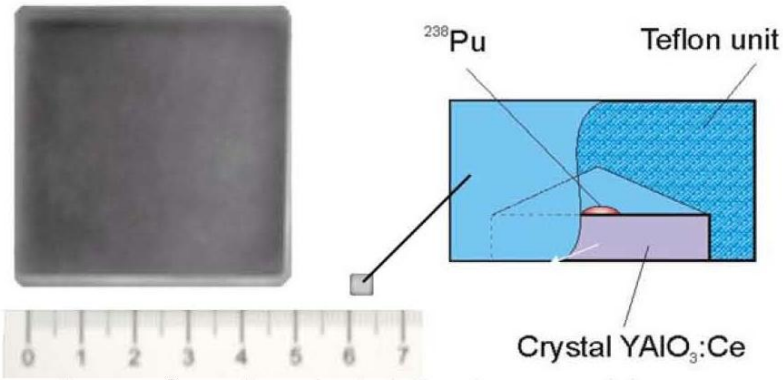

Fig. 7: *LS near small 5 x 5 cm^2 scintillator (on the left) and its principal design.*

Sources produced with different techniques were measured with silicon detectors and with plastic and liquid (only implanted sources) scintillators in order to check the quality as well as to study the responses of different detection schemes. The techniques used and the typical spectra obtained are shown in Fig. 8. Methodical studies at JINR showed that pure alpha sources of the isotopes listed in Table 3 can be successfully produced, and long-term tests were undertaken in order to investigate the practicability of monitoring and calibration with such sources.

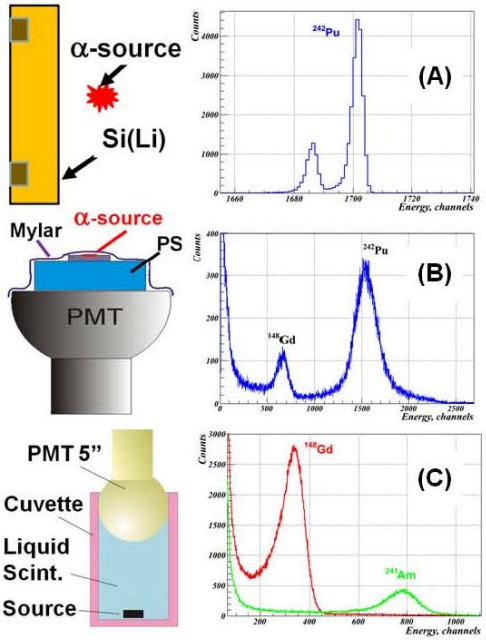

Fig. 8: *Source tests performed with Si(Li)-detectors (A), plastic (B) and liquid scintillators (C): schemes of test setup configurations as well as examples of spectra measured.*

The calibration and monitoring capsule was constructed in LSM and is shown in Fig. 9 The two EMS-implanted α-sources, ^{148}Gd and ^{241}Am (with activities ~2 Bq), were attached to the entrance face of the scintillator and the ^{238}Pu fueled light source (~20 Bq) was fixed to the side of the light guide. The capsule is hosted in a shielding box made of 10 cm of lead and 2 cm of copper. The setup is connected to one of the DAQ channels of the BiPo detector.

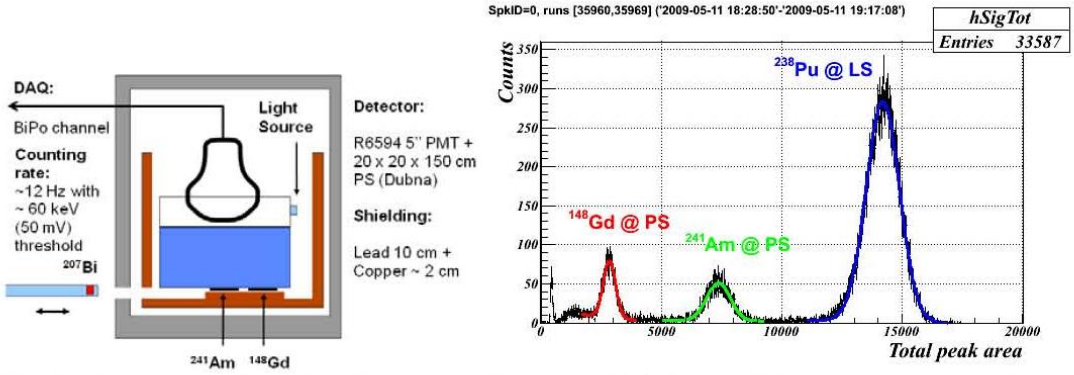

Fig. 9: *The test setup for calibration and monitoring at LSM (left) and A typical spectrum collected by the capsule during a one hour exposure (right).*

The calibration of the capsule was carried out with a ^{207}Bi source (total activity ~100 Bq). An open ^{207}Bi source, and the same source covered by a filter (electron stopper), were inserted successively in the calibration well (see Fig.9) for ~2 h. The spectra collected in both geometries were subtracted to obtain the ^{207}Bi β-spectrum. Internal conversion (IC) multiplet (IC K 976 keV) was fitted to obtain one calibration point (see Fig. 10). The second point was the zero of the energy scale, which was determined from a fit of the pedestal of the spectrum.

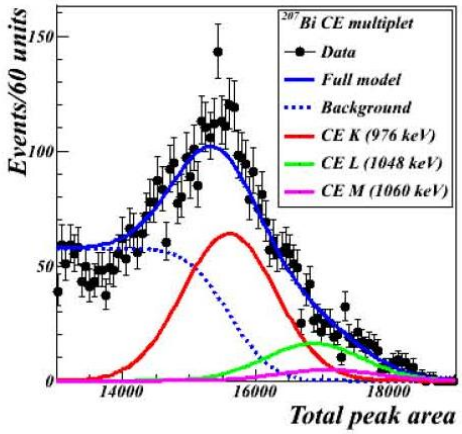

Fig. 10: *Fit of ^{207}Bi IC multiplet collected during calibration runs.*

A set of parameters was determined from experimental spectra collected by the capsule: intensities, positions and widths of all three peaks (^{148}Gd, ^{241}Am and LS with ^{238}Pu), and counting rates of different types of events (normal, under- and overflowing). These enable various cross-checks of the capsule operation to be made as well as demonstrating the monitoring capabilities of the method.

The variation in the positions of the peaks shown in Fig. 11 is a direct way to monitor the PMT gain. As one can see, the movement of all peaks is synchronous both in the smooth continuous flow, due to slow changes of experimental conditions, and in the characteristic jumps due to particular circumstances. The events which were easily recognized were ventilation problems in the laboratory, BiPo calibration, and hardware changes. In addition, the peak monitoring results are perfectly consistent with absolute ^{207}Bi calibrations. This means that once calibrated with an absolute source, the α-source peaks could be used as absolute references and not only as relative monitoring points.

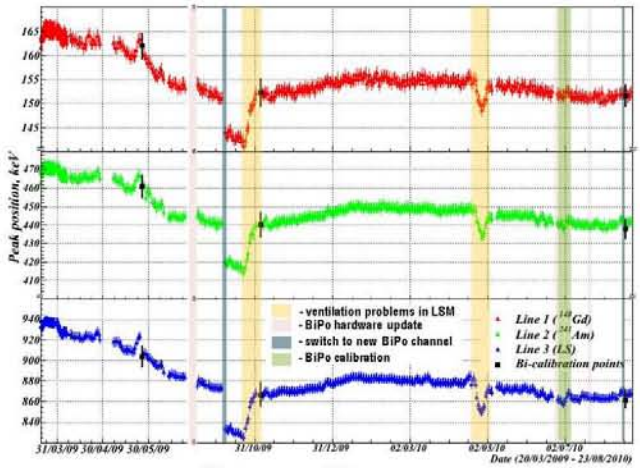

Fig. 11: *Movement of peak positions of ^{148}Gd (red), ^{241}Am (green), and LS (blue) with time.*

One can assume to a good approximation that long-lived α-sources produce a constant frequency signal in the time scale of the current measurement. This means that the measured absolute values of the source counting rates (CR) are sensitive to, and can be used to monitor, the dead time of a detection channel. One can see from the variation of source CR, shown in Fig. 12, that events such as hardware changes can be easily identified. Other slow changes of source activities are related to changes of experimental conditions (temperature, Radon, calibration, etc.).

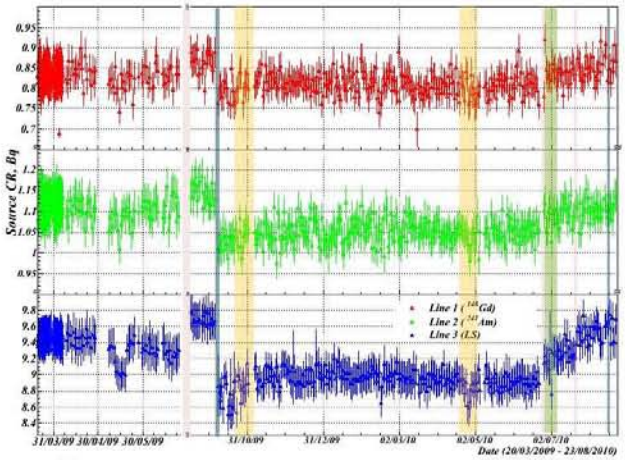

Fig. 12: *CR of ^{148}Gd (red), ^{241}Am (green), and LS (blue) with time.*

The position of the monitoring peak is usually chosen to be as close as possible to the region of interest (ROI) where the signal is registered or expected. As ROI are not the same for different experiments, the possibility of manipulating the positions of monitoring peaks would be a great advantage. Un fortunately, this is not possible for pure α-sources where the peak position is fixed and is determined by the energy of the α-particle and quenching of the scintillator. On the contrary, the peak position of the LS can be manipulated relatively easily. Simple modification of the light collection scheme leads to a change of the peak position over a wide energy range [0.8,2.3] MeV (see Fig. 13). This effect is most probably driven by differences in the light emission/absorption spectra of the PS, $YAlO_3$, and light guide (PMMA) convoluted in different combinations. An additional degree of freedom is the choice of scintillator used in the LS. The currently used $YAlO_3$ might be replaced with other scintillator (CsI, NaI, BGO, etc.) with a different quenching and scintillation decay constant.

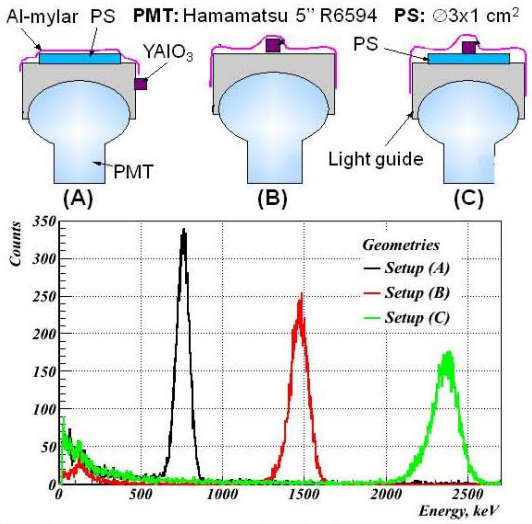

Fig. 13: *Different light collection schemes with a LS (top) and resulting LS spectra (bottom).*

In conclusion, a method to monitor and calibrate calorimeters in low background experiments using alpha sources has been developed. This is an important part of SuperNEMO R&D program. The viability of the method has been proven in a long term test measurement conducted in LSM. It is extremely important that various changes of the experimental conditions have been successfully tracked by the monitoring system.

SuperNEMO R&D program for 2011 will be concentrated on building of a demonstrator module replacing NEMO3 setup at LSM.

TGV

The goal of the experiment TGV is to search for neutrino-less and two-neutrino double beta decay processes ($\beta^+\beta^+$, β^+EC, EC/EC) of ^{106}Cd using a low-background and high efficiency spectrometer TGV-2 (Telescope Germanium Vertical). The detector part of the TGV-2 is composed of 32 HPGe planar type detectors with the sensitive volume of 2040 mm^2 x 6 mm each (about 3 kg of Ge). The total sensitive volume of detectors is as large as 400 cm^3. The detectors are mounted one over another together with double beta emitters in a common cryostat. Double beta emitters are 16 foils of ^{106}Cd with a thickness of 50 μm and a diameter of 52 mm inserted between the entrance windows of neighboring detectors. The distance between detectors and emitters were about 1.5 mm. The energy resolution of the detectors ranged from 3.0 to 4.0 keV at 1332 keV (^{60}Co). The total efficiency of the TGV-2 spectrometer is 50-70% depending on the energy threshold. The detector part of the TGV-2 (Fig. 14) was surrounded by copper shielding (>20 cm), a steel airtight box against radon, a led shielding (>10 cm), and an antineutron shielding made of borated polyethylene (16 cm).

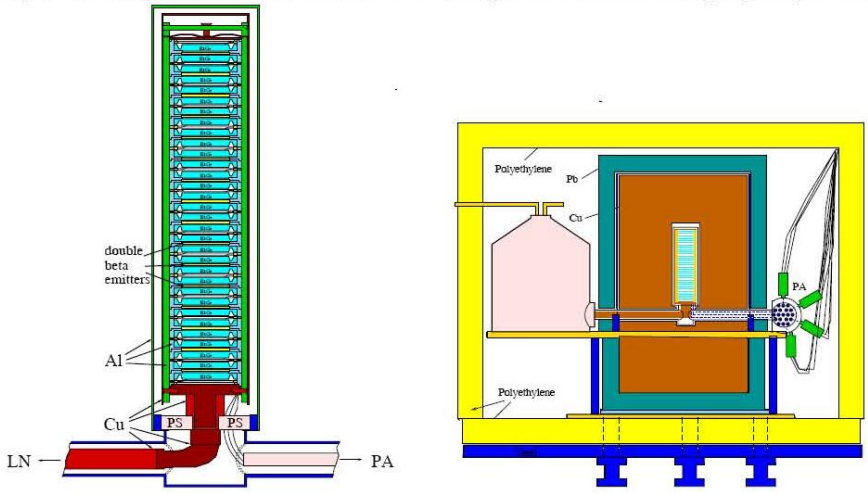

Fig. 14: *The detector part of TGV-2 spectrometer (left) and it in the passive shield.*

In 2010 results of long investigation started at 2005 have been published. The coincidences between two characteristic KX- rays of Pd detected in neighboring detectors were analyzed to search for 2νEC/EC decay of ^{106}Cd to the ground 0^+ state of ^{106}Pd (Fig. 15).

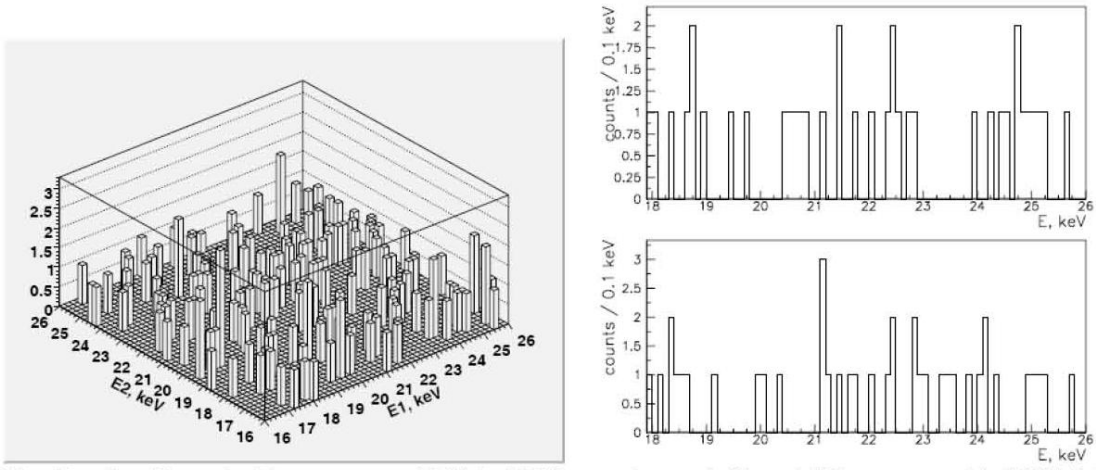

Fig. 15: *Double coincidence events (DC) in TGV experiment (left) and DC spectra with KX(Pd) in one of detectors (right).*

The search for 0νEC/EC resonance decay of ^{106}Cd to the 2741 keV excited state of ^{106}Pd was based on the analysis of KX(Pd) – γ 2741 keV and KX(Pd) – γ 2229 keV- γ 512 keV coincidences. Investigation of other branches of ^{106}Cd decay - 2νEC/EC decay to the 2^+,511.9 keV and 0^+_1, 1334 keV excited states of ^{106}Pd, $2\nu\beta^+$/EC and $2\nu\beta^+\beta^+$ decays to the ground and excited states of ^{106}Pd were based on the analysis of KX-511 keV, KX-622 keV, 511 keV-511 keV and 511 keV – 622 keV coincidences. Published limits on half-lives of double beta decay of ^{106}Cd are presented in Table 4.

Table 4: *The limits on half-lives of double beta decay of ^{106}Cd determined by TGV experiment.*

Decay mode	Transition to	$T_{1/2}$, 10^{20} y (C.L. 90%)
2νEC/EC	0^+, ground state 2^+,511.9 keV 0^+_1, 1334 keV	4.1 0.63 0.52
0νEC/EC	1,2+, 2741 keV	1.6
$2\nu\beta^+$/EC	0^+, ground state 2^+,511.9 keV 0^+_1, 1334 keV	1.1 1.1 1.6
$2\nu\beta^+\beta^+$	0^+, ground state 2^+,511.9 keV	1.4 1.7

Received by TGV experiment results for 2νEC/EC decay of ^{106}Cd to the ground 0^+ state of ^{106}Pd are more than 2 orders of magnitude higher than those obtained in other experiments and reached theoretical predictions ranging from 1.0×10^{20} to 5.5×10^{21} y.

Main publication in 2010: N.I. Rukhadze et al., Bulletin of the Russian Academy of Sciences: Physics, 74, 6 (2010), p821-824; N.I. Rukhadze et al., Journal of Physics: CS, 203, 012072 (2010) p1-3

Other activities and smaller experiments:

Neutron background study in LSM

An unbiased interpretation of results of experiments conducting at LSM requires a detailed understanding of all background sources. In the near future, it is planned to enlarge LSM to host the next generation of experiments searching for Dark Matter and $0\nu\beta\beta$. These will require further background reductions and a precise knowledge of the remainder. As part of the program of precise neutron background's study at LSM JINR group in frame of the JOULE agreement operates 2 sensitive detectors of thermal and fast neutrons. In previous year a significantly large neutron flux has been observed in the tambour region of LSM with respect to other places of the laboratory. One possibility of higher neutron flux is higher water content of rocks in this location. In such a case changes of neutron flux correlated with moon tides has been reported for another underground facilities. To check this for LSM long measurements were started with neutron detection system at the tambour region in November 2010.

Another use of ultra-sensitive neutron detector was in study of neutron flux inside of EDELWEISS2 shields (Fig 16). After long data taking (274 days of data accumulated) started in end of year 2008 and finished at May 2010, thermal neutron flux detected inside of the shields has been found to be $7.3\pm1.8 \times 10^{-9}$ neutron /cm^2 /sec (Fig 17). This is first independent measurement of neutron flux in close proximity to detectors of running Dark Matter search experiment. Yet another use of the detector was in measurement of neutron flux inside the shield when strong neutron source has been installed in different places around the shield (Fig. 18). In this way performance of the shield has been directly verified.

Fig. 16: *Photo of the ^{3}He filled proportional counter installed at close proximity to the EDELWEISS-2 cryostat.*

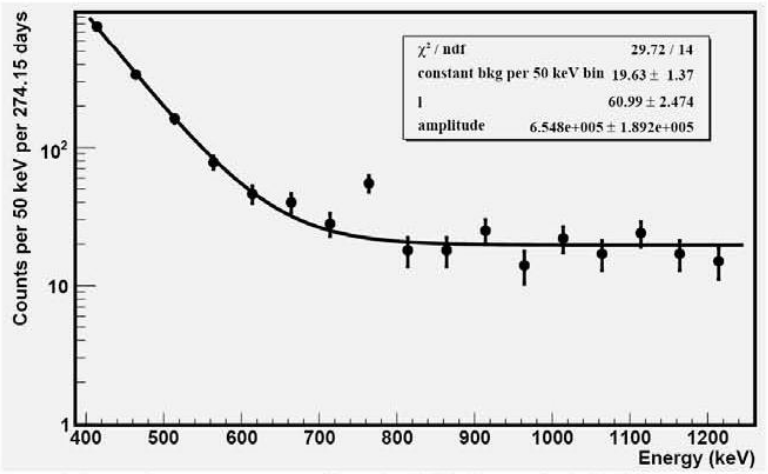

Fig. 17: *Experimental spectrum corresponding to 274 days of statistic accumulated with neutron detector installed inside of EDELWEISS2 shields. The neutron peak (764 keV) is clearly visible in the spectrum.*

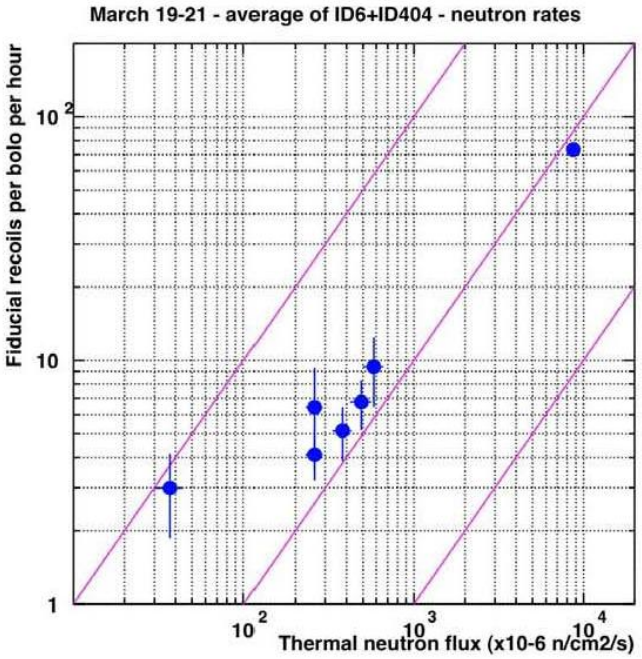

Fig. 18: *Correlation between thermal neuron flux measured inside of EDELWEISS2 shields and recoil rate registered with Ge detectors. The measurements performed with strong AmBe neutron source installed in different locations outside of the shields.*

Detector of fast neutrons installed in LSM was continuously used for monitoring of day by day stability of the neutron flux (Fig 19). In middle of 2010 the detector had problem with HV power supply which has been repaired by JINR group.

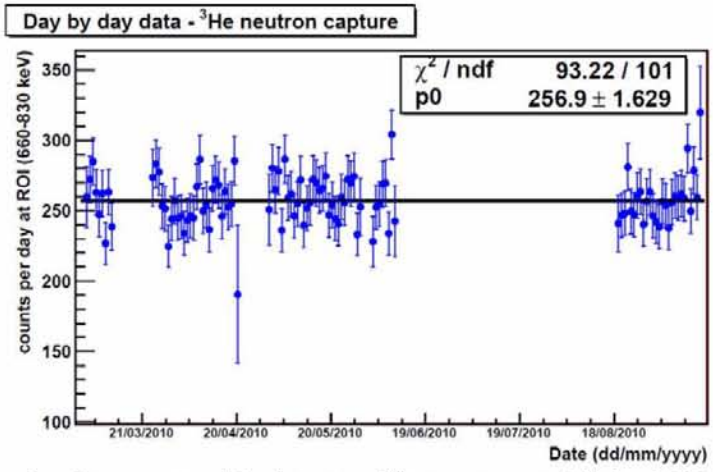

Fig. 19: *Day by day data registered by detector of fast neutrons in LSM in 2010*

We also performed new measurements in the SAS, tambour region of LSM. Motivation of this measurement become higher rate observed previously with both thermal and fast neutron detectors in the SAS region. It was 2-3 times higher with respect to the main hall of the lab. To identify source of neutrons, 2 holes were drilled in SAS walls. One on the Italy and one on the France side. Measurements were performed in both holes. We also repeated measurements in SAS region, approximately in the same point as old measurements.

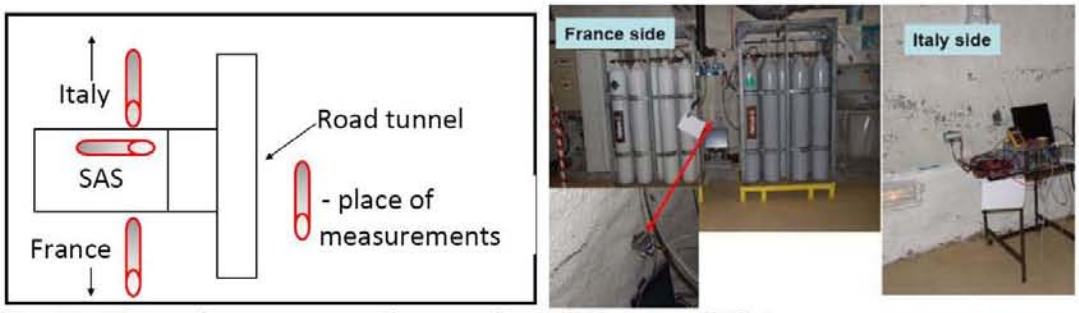

Fig. 19: *Places of measurements of neutron flux in SAS region of LSM.*

Results of measurements are:

Old measurement

Italy side 131 ± 12 cpd (live time = 0.89 days)

Measurements in June 2010

France hole 162 ± 9 cpd (all counts = 306, live time = 1.89 days)

Italy hole 191 ± 12 cpd (all counts = 238, live time = 1.25 days)

Italy side 140 ± 7 cpd (all counts = 362, live time = 2.58 days)

Measurements in August 2010

Italy hole 172.5 ± 4.6 cpd (all counts = 1416, live time = 8.21 days)

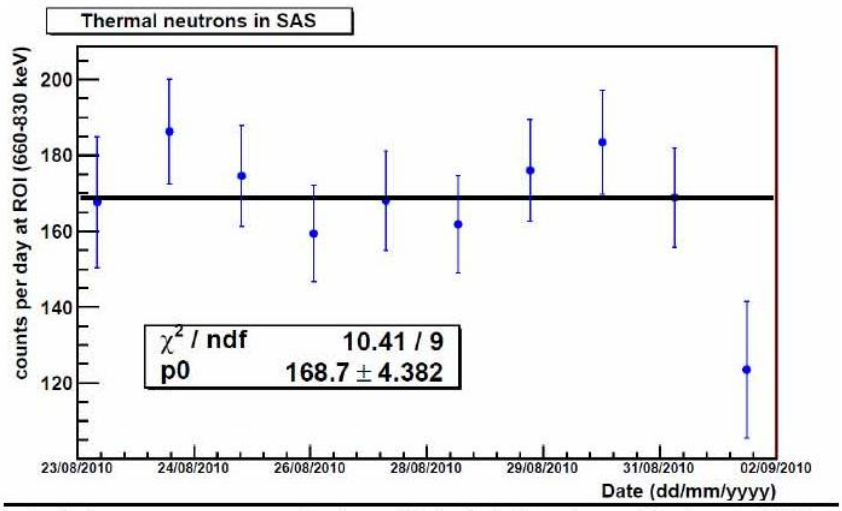

Fig. 20: *Relatively long measurements in place "Italy hole" performed in August 2010.*

New results are in agreement with previous measurement. It is important that in both holes measured thermal neutron flux is higher with respect to SAS. It seems that source of neutrons is located inside of walls, means in rock and concrete plus may be in water bringing radon, or just due to higher level of radon. In August we did relatively long measurements in the hole on the Italy side (Fig. 20). The reason of this measurements was attempt to find correlation of neutron flux and radon's tides due to moon, so correlation between neutron flux and moon elevation. Such correlations were recently reported in neutron measurements performed in Baksan neutrino observatory. Experimental data has been selected dependently from moon elevation angle. If consider sum of all data when moon elevation was positive and negative we will found for positive elevation: 7.12±0.25 counts per hour and for negative 6.42±0.25 counts per hour. These numbers are differ by 10%, effect if 2 sigmas. We continued this study in December 2010 in order to accumulate higher statistic. The data is under analysis.

Summary of all works performed at 2010 for neutron flux study at LSM:

1) Measurement of neutron flux inside of EDELWEISS2 shields;
2) Estimation EDELWESS2 shield performance with measurement with detector installed inside of shields and strong AmBe neutron source set in different locations outside of the shield;
3) Delivery of new acquisition electronics for detector of fast neutrons;
4) Investigation of high neutron flux problem in SAS region of LSM;
5) Long monitoring of neutron flux at LSM with both available detectors.

Publication in 2010: S. Rozov et al, Izvestiya RAN, 74, 4 (2010), in russian

Low activity measurements at LSM

The main activity has been connected with delivery of new high volume HPGe detector to LSM. The detector will be designated for certification of materials for SuperNEMO/EDELWEISS3/Eureca projects.

- Producer of the detector: Canberra-Packard;
- Type: coaxial P type germanium EGPC 160-240-R (with charge sensitive preamplifier);
- Relative efficiency: 160%; FWHM for 1.33 MeV γ-line <=2.4 keV; FWHM for 122 keV: <= 1.4 keV.

The detector has been delivered on the site in November 2010. Work on it installation and commissioning has been started.

Another activity accomplished in 2010 was repairing of HPGe detector at LSM. EURISYS MESURES EGSP 2500-R HPGe detector has been repaired and commissioned for use. It has HPGe crystal 290 g and can be efficiently used in LSM for low background study. The detector is shown on the Fig. 21.

Fig. 21: *Eurisys EGSP 2500-R detector.*

For test the detector performance we put it inside of modified EDELWEISS1 shield. This shield has been used before 2002 for dark matter search with cryogenic germanium bolometers. For this purpose an ^{3}He-^{4}He dilution cryostat was set inside of the shield with 3 Ge detectors as shown on the Fig. 22. Achieved level of background is shown on the same figure.

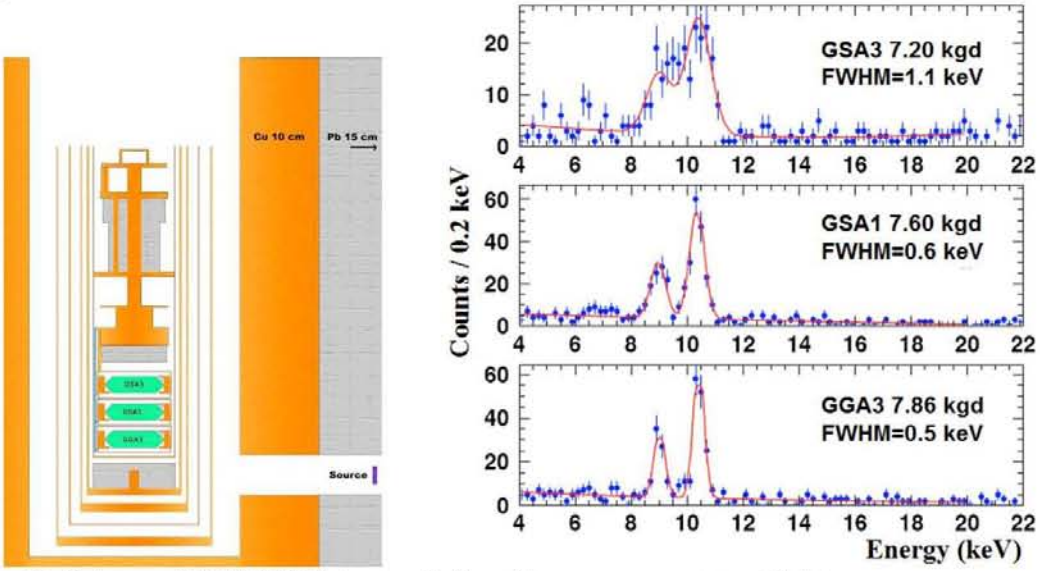

Fig. 22: *Scheme of EDELWEISS-1 setup (left) and low energy spectrum (right).*

As we can see form the fig. 22, level of background in 4-8 keV region was found to be 3-4 events per kgd on world leading level. For test repaired detector EDELWEISS-1 shield has been reconstructed in the way that cryostat with detector inserted into the shield through the opening designated originally for entry of calibration sources (Fig. 22). Upper part of the shield has been closed with cupper plates (not less of 10 cm) and by lead (about 20 cm) (Fig. 23).

Fig. 23: *View from the top of EDELWEISS1 shield (left) and photo of process of positioning of cupper plates on the top (right).*

The entry hall has been shielded by cupper and lead, as partly shown on the Fig. Additionally radon free air supply (below of 10 mBq/m^3) to the detector surrounding has been made.

Fig. 24: *View of the shield from side of cold finger, on the left – cupper shield, on the right – lead shield with pipe of radon-free air supply.*

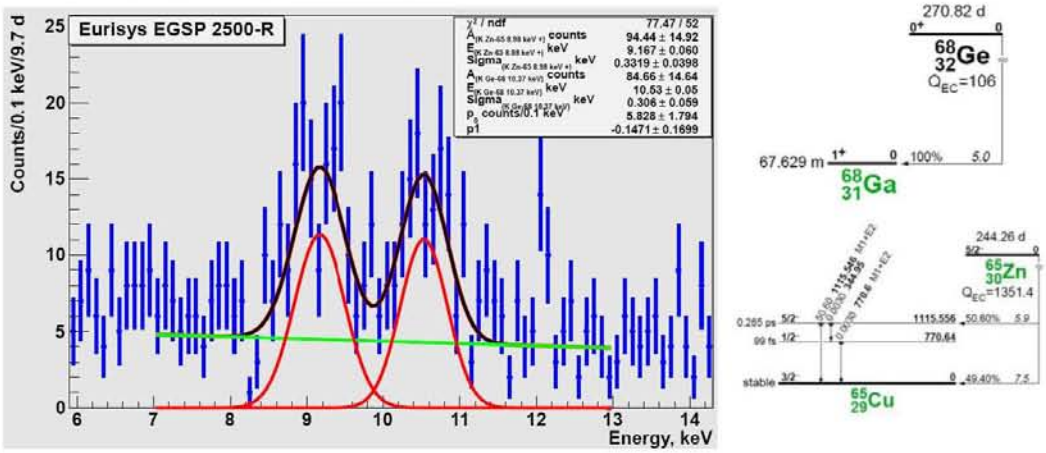

Fig. 25: *Experimental spectrum from 6 to 14 keV and decay schemes from which observed lines are arising.*

Output signal from detector's preamplifier has been input to the Canberra 2022 shaping amplifier. Shaped signal has been digitized with 12 bit adc of JINR production. For all events with amplitude above of a discriminator threshold the event arrival time (PC time) and amplitude were recorded to a file. The energy scale of the detector has been calibrated with 53 keV and 80 keV γ-lines from decay of ^{133}Ba. Linearity of the scale in low energy region (close to the threshold) has been checked with cosmogenic lines shown on the Fig. 25. Most intense lines in region below of 15 keV are arising due to electron capture decay of ^{68}Ge and ^{65}Zn to the ground states. Energies of these lines are equal to K electron binding energies in gallium 10.367 keV and in cupper 8.979 keV.

Accumulated data show that energy threshold is about 2 keV. Energy resolution (FWHM) for 10.37 keV line is 700 eV. All spectrum accumulated during 10 days of measurements in December 2010 is shown on Fig. 26. There are 2 noticeable lines in the spectrum: 46.5 keV γ-line from decay of 210Pb and K X-rays of lead with energies from 72 keV (most intense line is 75 keV $K_{\alpha 1}$)

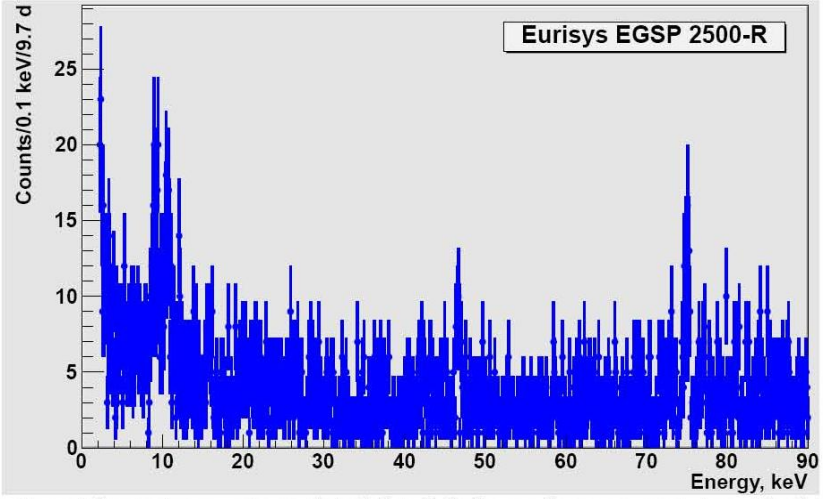

Fig. 26: *Experimental spectrum accumulated for 9.7 days of measurements with detector Eurisys EGSP 2500-R in modified EDELWEISS-I shield.*

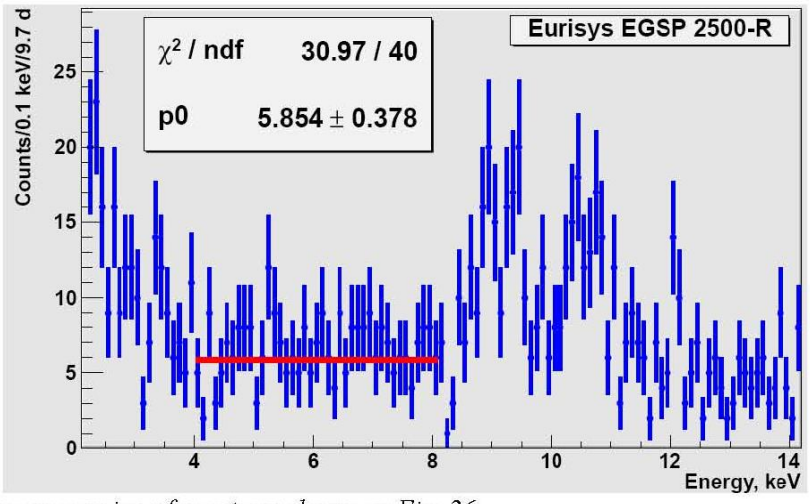

Fig. 27: *Low energy region of spectrum shown on Fig. 26.*

With taking into account weigh of the detector, background in the region of 4 to 8 keV has been found to be about 20 counts per 1 kgd. This is only about 5 times higher with respect to EDELWEISS-1 detectors. This is an excellent result for commercial detector. In general our tests demonstrated capability of using of the repaired detector for low background investigations in LSM.

Study of polyethylene as common material for neutron shields

JINR and LSM conducted extensive work for analysis of radioactive properties of polyethylene (PE): material which has a wide use as neutron shield in many low background experiments (in particular in EDELWEISS-2 conducting in LSM). Our first aim was estimation of own neutron background produced inside of PE. A possible sources of neutrons inside of PE are: SF of uranium and α-n reaction on ^{13}C. C-13 is isotope presented in nature with natural abundance 1.1%. Since PE formula is CH2, this means that normal PE contains C-13. It should be noted: alpha-n reaction is not possible on C-12 (for alphas from natural radioactive chains). There are following sources of alphas in polyethylene:

1) Natural contamination by uranium and thorium, in particular ^{238}U decay chain and ^{232}Th decay chain. ^{238}U chain has 8 alphas and ^{232}Th chain has 6 alphas with energies up to 8.8 MeV. Polyethylene (PE) has some internal contamination by both ^{238}U and ^{232}Th.

2) ^{222}Rn. Usually any shield is in contact with air containing radon-222. For example, EDELWEISS-2 neutron shield is surrounded from all sides (include internal one) with air level of radon of which is about 10 Bq/m^3. Radon can diffuse inside of PE. Radon decays by alpha. All it daughters can escape from PE only due to recoils after alpha decay. Depth of such escape zone is about few tenth nm. Thus radon diffusion can increase neutron yield due to alpha-n reaction.

3) Radon daughters sticking to surface. Radon daughters are also radioactive but are not gases in normal laboratory conditions, thus in additional to diffusion will tends to accumulation on surfaces.

First we have to start from calculation of neutron yields for alphas in PE. Standard (table of isotopes) energies of alphas and branches ratios were taken. dE/dX for alphas in PE was calculated with SRIM code and shown in Fig 28.

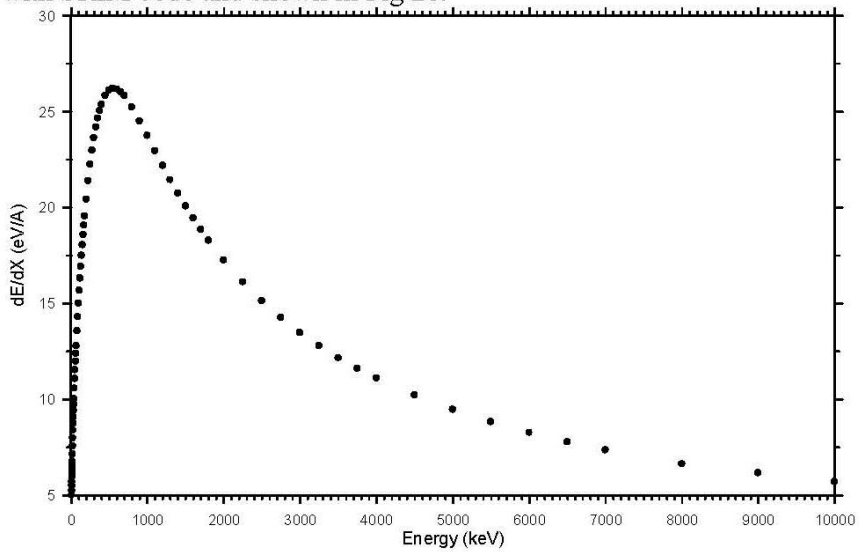

Fig. 28: *dE/dX for alphas in PE*

Cross section of reaction alpha-n on C-13 was taken from [S. Harissopulos et al., Phys. Rev. C 72, 062801(R) (2005)] and shown in Fig. 29.

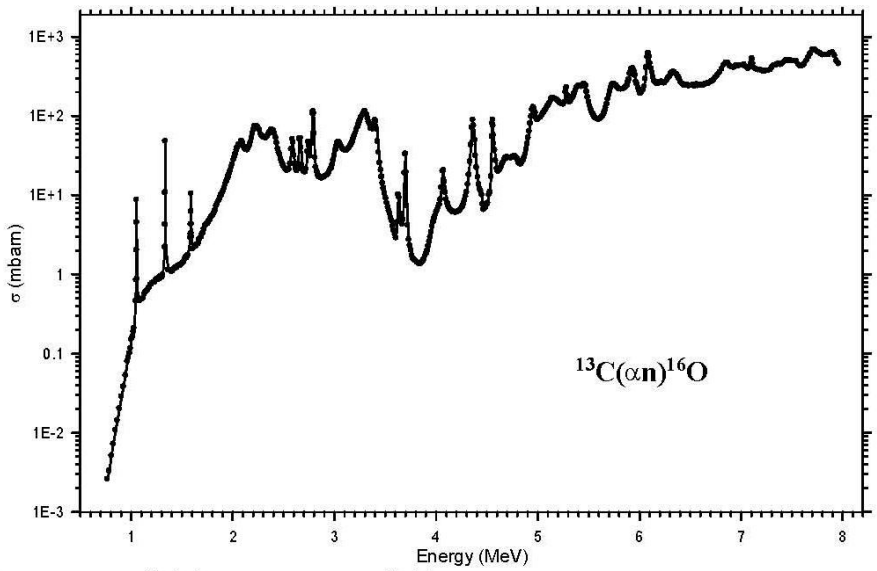

Fig. 29: *Cross section of alpha-n reaction on C-13*

With above data integral probabilities of neutron emission per 1 alpha were calculated for all alphas in both ^{238}U and ^{238}Th chains.

^{238}U chain:

Isotope	**Alphas' energy (branch)**	**Probability of neutron emission per 1 alpha**
^{238}U:	4198 (79%)	$2.38\ 10^{-8}$
	4151 (20.9%)	$2.37\ 10^{-8}$
^{234}U:	4774.6 (71.38%)	$3.01\ 10^{-8}$
	4722.4 (28.42%)	$2.89\ 10^{-8}$
	4603.5 (0.2%)	$2.74\ 10^{-8}$
^{230}Th:	4687.7 (76.3%)	$2.89\ 10^{-8}$
	4621.2 (23.4%)	$2.79\ 10^{-8}$
^{226}Ra:	4784.38 (94.45%)	$3.02\ 10^{-8}$
	4601.7 (5.55%)	$2.77\ 10^{-8}$
^{222}Rn:	5489.5 (99.9%)	$7.59\ 10^{-8}$
^{218}Po:	6002.4 (100%)	$1.29\ 10^{-7}$
^{214}Po:	7686.8 (100%)	$4.99\ 10^{-7}$
^{210}Po:	5304.4 (100%)	$5.69\ 10^{-8}$

Probability of neutron emission from U-238 chain:
sum of all: $8.7\ 10^{-7}$ per 1 decay of ^{238}U in case if the chain is in equilibrium and not broken
sum (^{222}Rn and after): $7.04\ 10^{-7}$ per 1 decay of ^{222}Rn
^{218}Po + ^{214}Po: $6.28\ 10^{-7}$
^{214}Po alone: $4.99\ 10^{-7}$
SF (^{238}U): $5.45\ 10^{-7}$ * 2.2 n/SF = $1.2\ 10^{-6}$ per 1 decay

Isotope	Alphas' energy (branch)	Probability of neutron emission per 1 alpha
^{232}Th:	4013 (77.9%)	$2.3\ 10^{-8}$
	3954 (22.1%)	$2.3\ 10^{-8}$
^{228}Th:	5423.2 (71.1%)	$6.8\ 10^{-8}$
	5340.3 (28.2%)	$6.0\ 10^{-8}$
	5211 (0.435%)	$4.9\ 10^{-8}$
	5173 (0.235%)	$4.7\ 10^{-8}$
^{224}Ra:	5685.4 (94.9%)	$8.7\ 10^{-8}$
	5448.7 (5.1%)	$7.1\ 10^{-8}$
^{220}Rn:	6288.1 (99.9%)	$1.77\ 10^{-7}$
^{216}Po:	6778.3 (100%)	$2.54\ 10^{-7}$
^{212}Bi: *0.359		
	6089.9 (27.1%)	$1.44\ 10^{-7}$
	6050.8 (69.9%)	$1.35\ 10^{-7}$
	5768 (1.8%)	$9.6\ 10^{-8}$
	5626 (0.2%)	$8.4\ 10^{-8}$
	5607 (1.2%)	$8.3\ 10^{-8}$
^{212}Po: *0.641		
	8784.4 (100%)	$8.78\ 10^{-7}$ (?) probably more, cross section above 7.9 MeV was taken as for 7.9 MeV

Probability of neutron emission from Th-232 chain:
sum of all: $1.22\ 10^{-6}$ per 1 decay of ^{232}Th in case if chain is in equilibrium and not broken

Uncertainties of above values come mainly from uncertainty of cross section which from different sources differs by 30%. We also calculated neutron's spectra for ^{222}Rn and its alpha decaying daughters in assuming isotropic distribution of neutrons (Fig. 32). It is known that this is not a case, because neutron emission is mainly happen by resonances. Precision of available experimental data on angle distribution is not very impressive, and in addition as was shown in [S. Enomoto, "Neutrino Geophysics and Observation of Geo-Neutrinos at KamLAND", PhD thesis, chapter 6, Tohoku University, (2005)] principal behavior of neutron spectrum has no dramatically dependence from angles (Fig. 30).

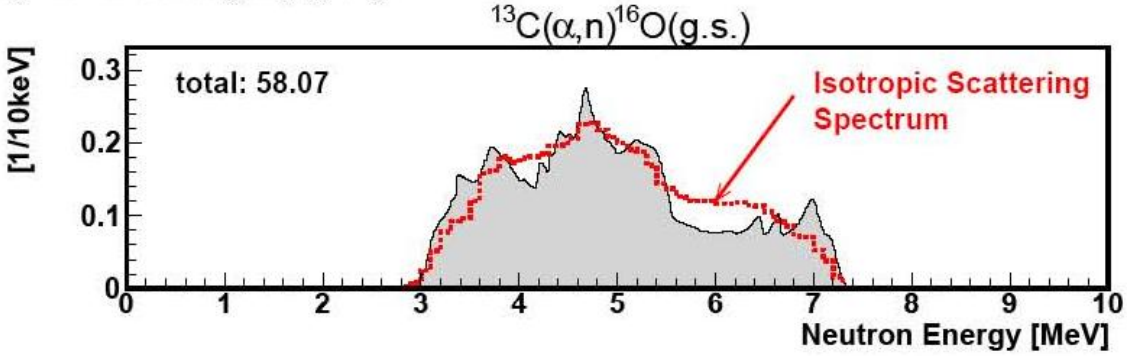

Fig. 30: *Neutron energy spectrum due to alpha-n reaction in pseudocumene based liquid scintillator.*

Also, in our calculations neutron production to excited states in ^{16}O was ignored, but it has been noted that such production has place and became dominant for high energies. This will change neutron spectrum corresponding to alphas with energies above of 5.5 MeV (as shown on Fig. 31)

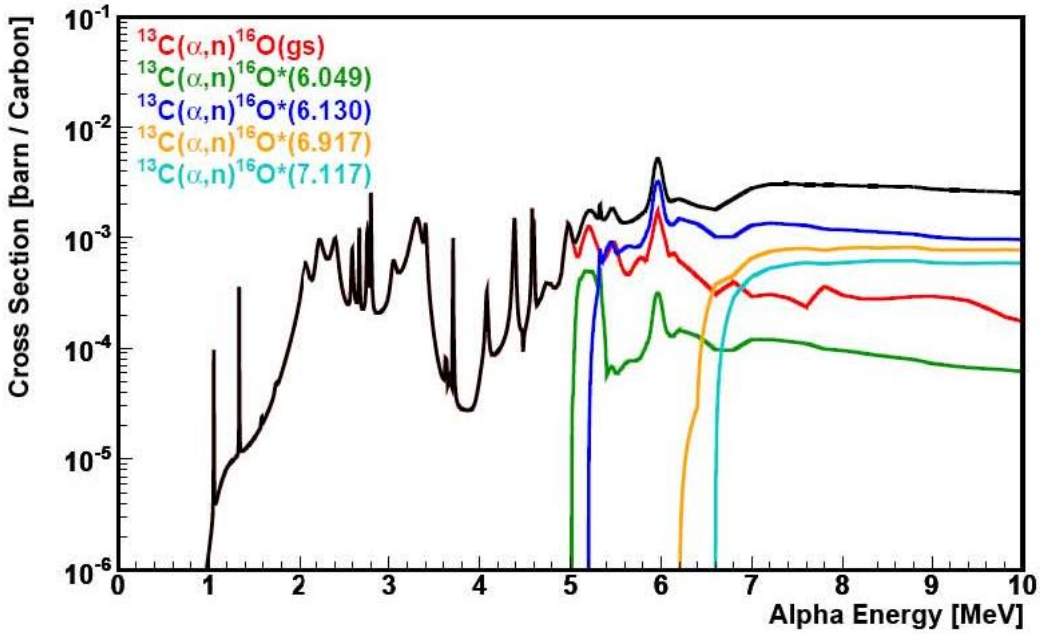

Fig. 31: *$^{13}C(\alpha,n)^{16}O^*$ cross section from JENDL data set.*

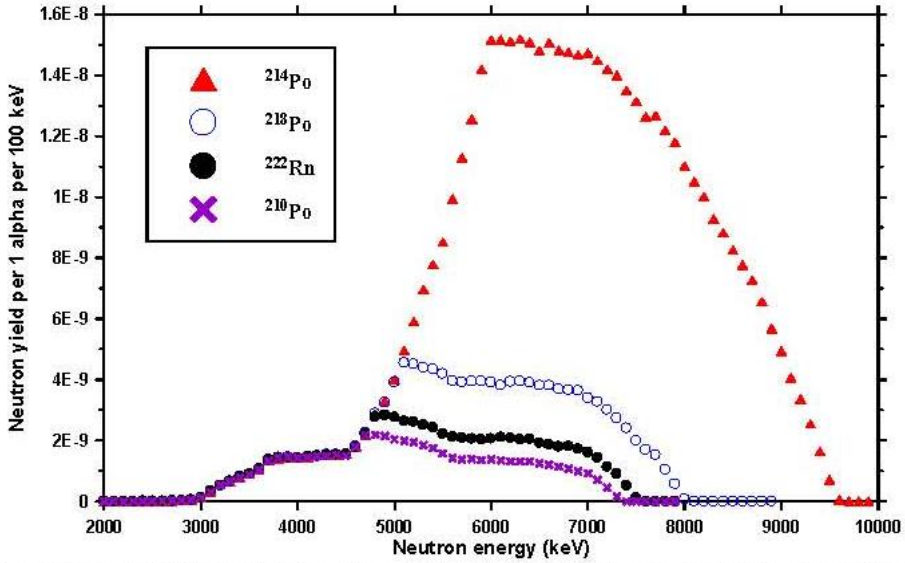

Fig 32: *Absolute probabilities of neutron's emission with different energy due (□,n) reaction in PE for radon-222 and it alpha radioactive daughters.*

To make analysis of received data radon diffusion into PE has to be considered. Radon diffusion was estimated with using standard approach [M. Wojcik et al, Nuclear Instruments and Methods in Physics Research A 449 (2000) 158-171]. Diffusion coefficient was taken as $D = 4.3 \cdot 10^{-12}$ m^2 s^{-1} from [M. Durcik and F. Havlik, Journal of Radioanalytical and Nuclear Chemistry, Articles, Vol. 209, No. 2 (1996) 307-313]. Radon solubility in PE was taken equal 1 (which is may be not a case). Distribution of radon inside of PE is shown on Fig. 33.

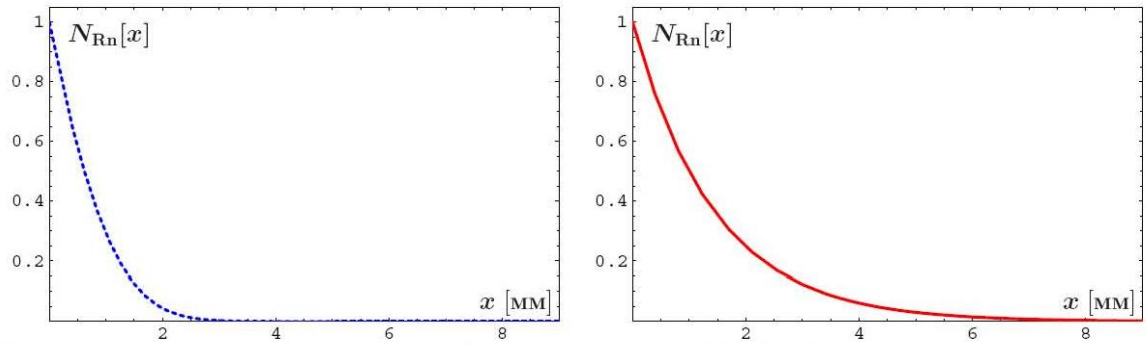

Fig. 33: *Concentration of radon under different depths inside of PE. Surface concentration is taken to be 1. Left picture: 1 day after start of diffusion. Right one: $t \to \infty$. Please note that surface concentration can be greater (or lower) than air one in case if the solubility is above (less) of 1. Please also note that diffusion was experimentally estimated for thin membrane, diffusion coefficient for a bulk of PE can be significantly different (larger).*

So, the conclusion can be made based on received characteristic radon diffusion length in PE 1.5 mm. With external radon level in 10 Bq/m^3 1 m^2 of PE will have 0.015 Bq of ^{222}Rn. Neutron yield from ^{222}Rn and it daughters will be 1.1 10^{-8} per m^2 per sec.

To find out neutron yield from natural contaminations (uranium and thorium) we have to estimate it content inside of PE. For PE from EDELWEISS-2 shield this has been performed with help of neutron activation analysis. By our requestsuch analysis has been performed by our colleagues I.I. Sadikov, A.V.Rakhimov and M.I. Salimov in Institute of Nuclear Physics of Uzbek Academy of Sciences (Tashkent, Uzbekistan) in December 2010. The part of polyethylene (standard block) has been taken from LSM in spring 2010. 4 samples were prepared, hereinafter referred as n1, n2, n3 and n4. Samples n1 and n2 were used for relatively long activation and n3 and n4 for shorter one.
Results of long activation: Samples n1 and n2 with m_{n1}=10.4540 g and m_{n2}=10.4147 g were putted into aluminum container closed with special epoxy glue. The polyethylene (PE) samples were irradiated by neutrons with flux 1·10^{14} n·cm^{-2}·sec^{-1} during 48 hours in the second channel of BBP-CM nuclear reactor. This irradiation was started at 10h50 am on December 1st 2010. 13 hours after irradiation samples were taken out from the containers, wiped by 0.1 M of hydrochloric acid and deposited into radioactive clean special paper bag. These samples were investigated by means of gamma spectrometry (December 14, 2010). Results presented in the table 5.
Results of short activation: Samples n3 and n4 with m_{n3}= 0.9900 g and m_{n4}= 1.0358 g were irradiated in the same way as samples n1 and n2 but during only 5 h and in additional each container inside had K, Th and U etalon samples. This activation had place December 10th, 2010, from 10 pm. 3 days after the activation samples and etalons were investigated by mean of gamma spectrometry. Results of analysis are presented in the table 6. It is interesting that sample n3 was found to have almost 3 times higher contamination by U with respect to the all other samples. At this time we don't know nature of this disagreement and we don't exclude that this is real higher contamination of this particular sample.

Our investigations confirm results of low background gamma measurements that polyethylene has uranium contamination on ppb and thorium contamination on 0.1 ppb levels. We found that contamination by potassium is relatively high. With taking into account that 40K(g/g)= 0.00012natK(g/g), potassium decay rate is 30 Bq/g. U and Th decay retas are: 238U (99.2745% abundance) decay rate is 12400 Bq/g and 232Th (100% natural abundance) decay rate is 4100 Bq/g. With taking into account values of U, Th and K contaminations in PE, U decay rate in PE is highest.

Table 5: Amounts of different elements found in polyethylene samples n1 and n2.

№	element	Content, (g/g)	
		n1	n2
1	As	$(2,37\pm0,16)\cdot10^{-9}$	$(3,21\pm0,16)\cdot10^{-9}$
2	Au	$(3,32\pm0,02)\cdot10^{-10}$	$(9,93\pm0,18)\cdot10^{-11}$
3	Ag	$(1,33\pm0,06)\cdot10^{-10}$	$(1,56\pm0,06)\cdot10^{-10}$
4	Br	$(7,51\pm0,12)\cdot10^{-9}$	$(9,13\pm0,13)\cdot10^{-9}$
5	Ce	$(1,64\pm0,02)\cdot10^{-9}$	$(2,04\pm0,03)\cdot10^{-9}$
6	Co	$(4,15\pm0,03)\cdot10^{-9}$	$(5,86\pm0,15)\cdot10^{-10}$
7	Fe	$(3,86\pm0,11)\cdot10^{-7}$	$(3,06\pm0,33)\cdot10^{-7}$
8	Hf	$(4,98\pm0,37)\cdot10^{-11}$	$(8,63\pm0,35)\cdot10^{-11}$
9	Mo	$(1,92\pm0,075)\cdot10^{-9}$	$(1,84\pm0,07)\cdot10^{-9}$
10	La	$(3,47\pm0,03)\cdot10^{-9}$	$(2,00\pm0,09)\cdot10^{-9}$
11	Re	$(5,17\pm0,01)\cdot10^{-8}$	$(1,26\pm0,01)\cdot10^{-8}$
12	Sb	$(2,83\pm0,01)\cdot10^{-8}$	$(3,68\pm0,01)\cdot10^{-8}$
13	Sc	$(2,70\pm0,04)\cdot10^{-10}$	$(1,46\pm0,03)\cdot10^{-10}$
14	Sn	$(2,49\pm0,06)\cdot10^{-8}$	$(1,40\pm0,05)\cdot10^{-8}$
15	Se	$(3,10\pm0,11)\cdot10^{-9}$	$(2,12\pm0,10)\cdot10^{-9}$
16	Ta	$(1,81\pm0,02)\cdot10^{-9}$	$(1,09\pm0,02)\cdot10^{-9}$
17	Th	$(1,16\pm0,04)\cdot10^{-10}$	$(8,39\pm0,90)\cdot10^{-11}$
18	U	$(1,24\pm0,04)\cdot10^{-9}$	$(7,97\pm0,41)\cdot10^{-10}$
19	Zn	$(9,98\pm0,28)\cdot10^{-6}$	$(1,03\pm0,03)\cdot10^{-5}$

Table 6: Amounts of K and U and limit on Th found in polyethylene samples n3 and n4.

№	Element	Content, (g/g)	
		n3	n4
1	K	$(1,60\pm0,35)\cdot10^{-7}$	$(1,03\pm0,25)\cdot10^{-7}$
2	U	$(3,06\pm0,20)\cdot10^{-9}$	$(1,22\pm0,15)\cdot10^{-9}$
3	Th	$1,05\cdot10^{-9}$	$9,59\cdot10^{-10}$

Assuming that neutrons can escape only from first 10 cm under PE surface we can find out that 1 ppb contamination of PE by ^{238}U will produce 2.6 10^{-6} neutrons per m^2 per sec. 0.1 ppb contamination of PE by ^{232}Th will produce 5.0 10^{-8} neutrons per m^2 per sec.

Another possible source of neutrons could be radon daughter stick to surface after radon decay in air. Let's assume that ^{218}Po does not stick to surface but ^{214}Po does stick before it alpha decay. We also assume that 1 m^2 of surface corresponds to 0.1 m^3 of air. Thus, concentration of ^{214}Po on surface of PE could be 1 Bq/m^2. This will produce 5 10^{-7} n/sec/m^2 emitting in all directions.

The summary is that main neutron source inside of PE is uranium contamination. The flux of neutrons can be as high as 2.6 10^{-6} neutrons per m^2 per sec for 1 ppb contamination of uranium. This fact must been taken into account in planning of future low background experiments. Radon and it daughters are also could be a dangerous source of neutrons, in general radon level has be under control even outside of gamma shields and as low as possible.

Radiochemical project for LSM:

In 2010 JINR and LSM started new cooperation for development in the LSM underground laboratory and in JINR a complex radiochemical programs for trace of ultra low quantities of natural radioactive elements. Results of the project will have a direct application for all physics experiments conducting at LSM for certification of construction elements and samples on its radioactive purities. The results will be as well required in time of building of the LSM extension. The program was started from exchange of "know-how" for building of ultra thin samples for alpha and beta spectrometry. Methods of purification of materials for future double beta decay experiments start to be developed.
One of the most important results in 2010 is new approach to method of selenium purification developed in collaboration between JINR and LSM radiochemistry groups. This is so called reverse method purification (Fig. 34). The method is based on work previously performed by JINR group [*A 44Ti/44Sc radionuclide generator for potential application of 44Sc-based PET radiopharmaceuticals October 2009 Radiochim.Acta 98 149-156 (2010) / Doi 10.1524 / ract.2010.1701*]. The method will be tested with natural selenium in 2011.

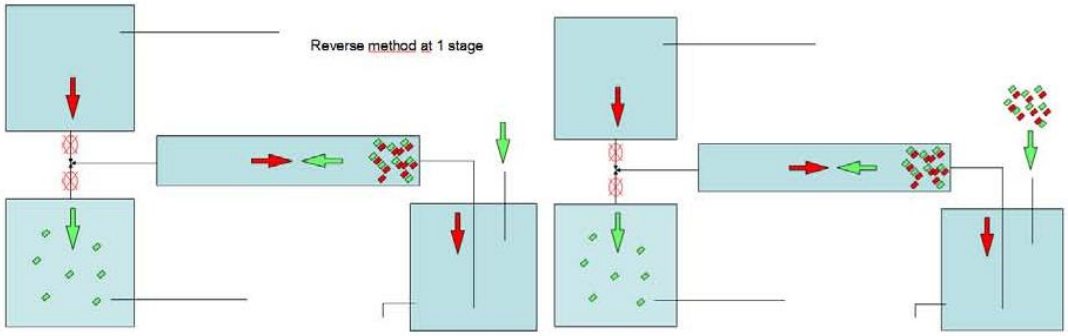

Fig. 34: *A schematic approach to the reverse method of purification.*

Radon measurements at LSM:

In 2007 JINR developed, build and delivered to LSM high sensitive radon detector. In 2008-2010 this detector was continuously used for control air environment at upper part of the EDELWEISS2 cryostat. This is one of the key information need for interpretation of EDELWEISS2 data. The general scheme of anti-radon protection of EDELWEISS2 experiment is shown on the Fig. 35.

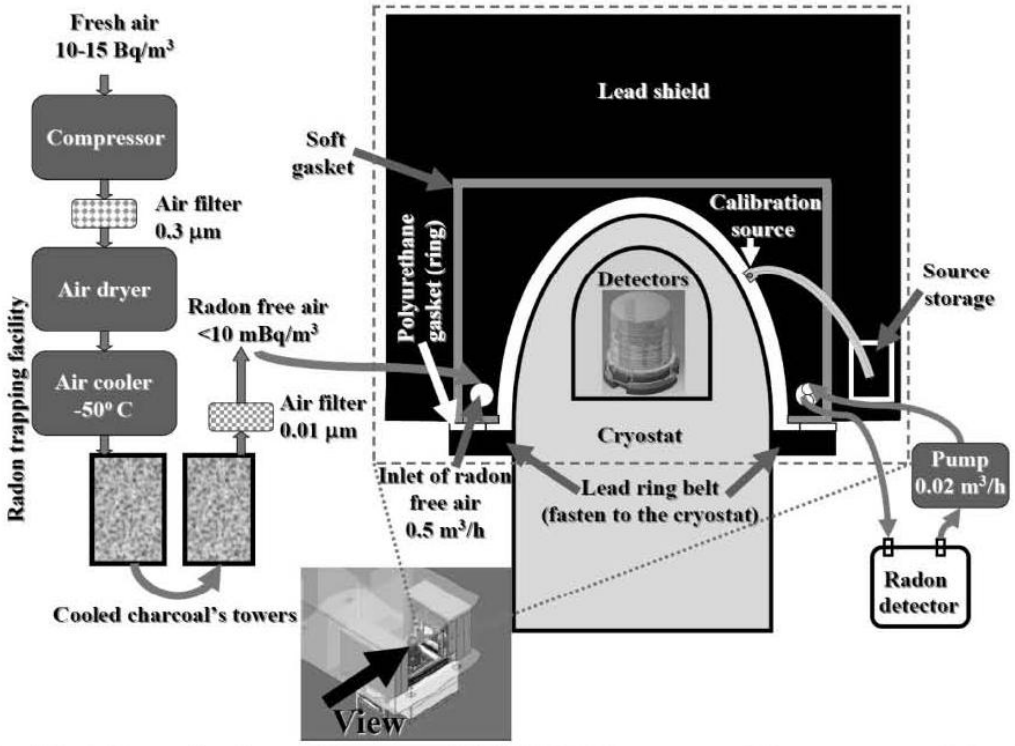

Fig. 35*: Scheme of radon environment of EDELWEISS2 cryostat. Only upper part of the shield is shown.*

In December 2010 the line connected the radon detector with cryostat environment has been extensively purified, as result own background of the radon detection setup has been reduced twice. We also continue to use the radon data for verification of proper closure of EDELWEISS2 shields. In 2010 several cases were detected when small gap remained between two parts of the shield, thus shield was not closed as expected. Thanks to radon data this situations were found quickly and shields were successfully re-closed. Importance of such control can not be underestimated for such experiment as EDELWEISS2 searching extremely rare events of WIMP-nucleon scattering.

Real-time SER characterization of SRAM memories:
Neutron-induced Single Event Effects (SEE) are now recognized as a major concern for the reliability of electronic devices in terrestrial environments. As one of the test platforms, since 2007 the permanent test equipment was installed in LSM to perform long-term and real-time SEE characterization of CMOS technologies. The second test platform has an altitude location on Plateau de Bure to strengthen natural neutron irradiation, thus providing a possibility to study the nature of SEE in more clear way. In 2010 the collaboration of Dubna group with IM2NP (Aix-Marseille University, team leader J.L. Autran) was continued. In particular, MC simulation of the neutron monitor PdBNM has been continued. Parallel measurements with JINR and IM2NP neutron detectors were performed at Aix-Marseille University to calibrate the system of neutron detection located at Plateau de Bure. The spectrum recorded with JINR CHM-57 neutron counter is shown on the fig. 36. The "neutron" peak 764 keV is clearly pronounced.

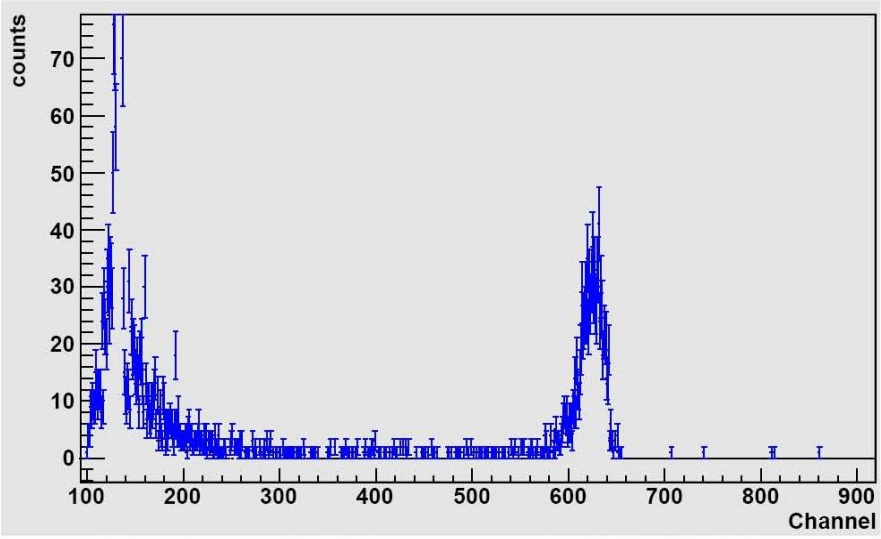

Fig. 36: *Experimental spectrum received in the measurements with the CHM-57 counter.*

Analysis of peak intensity was done by the region of interest (ROI) from 660 to 830 keV. For this particular region the sensitivity of the detector is 243 counts/sec for an isotropic (4π) thermal neutron flux at 1 neutron/cm^2/sec. 2 measurements were performed: one with naked counter (Fig. 37) and second one with the counter inside of the polyethylene (PE) tube (Figs. 38 and 39).

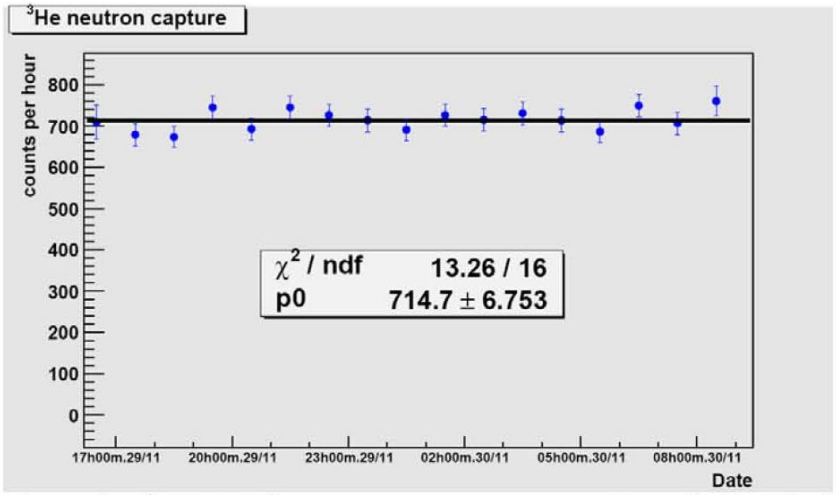

Fig. 37: *Rate detected with CHM-57 bare counter, measurements in Marseille 29-30/11/2010.*

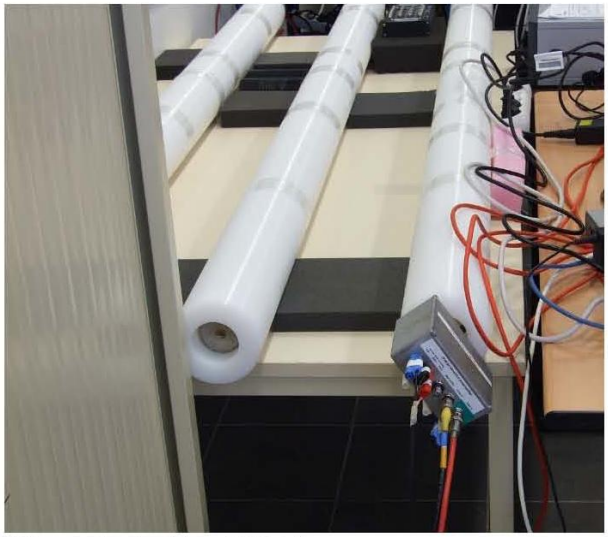

Fig. 38: *Photo of CHM-57 counter inside of PE tube.*

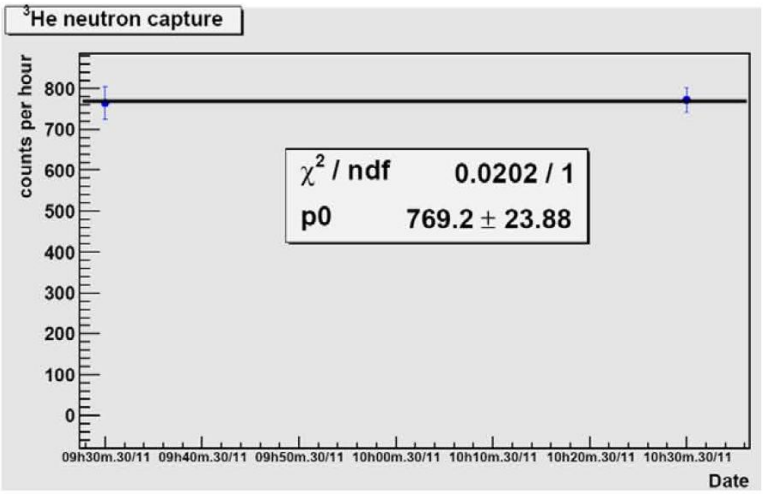

Fig. 39: *Rate detected with CHM-57 counter inside of PE moderator, measurements in Marseille morning 30/11/2010.*

Summary of results received with JINR detector is presented in the table:

	Date	Average N counts in ROI per 1 hour	Flux of thermal neutrons n/m^2/sec
Bare CHN-57 counter	4pm 29.11.2010 – 9 am 30.11.2010	715±7	8.2±0.1
CHM-57 counter in PE	9h30-10h30 am 30.11.2010	769±24	8.8±0.3

For Marseille detector (LND 253109) measurements were performed with detector inserted in the PE moderator tube. For measurements we used double pass shaping amplification. Received spectrum is shown on the fig. 40.

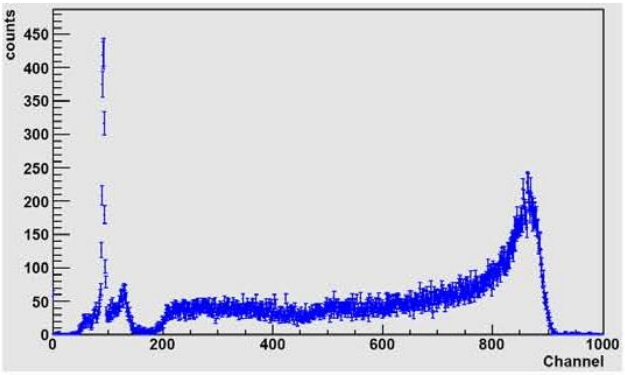

Fig. 40: *Experimental spectrum received in the measurements with the LND 253109 counter.*

As clear from the picture, the 764 keV peak is clearly pronounced but there is also a long tail going almost to 0. The reason of this tail seems to be due to "double pulse" structure of event's signals and then "not enough" time integration and thus not complete charge collection in each pulse. The main problem of extracting results from this spectrum is connected with high area of the tail. The tail could contain not only neutron events but also noise. Another potential problem with the spectrum is that it lowest energy part has been cut off by the discriminator's threshold. And we don't know what fraction of neutrons has been not measured. In this situation we took maximal measured spectrum from channel 170 to channel 940 for consideration. The integral rate detected with the detector is depicted on the Fig. 41.

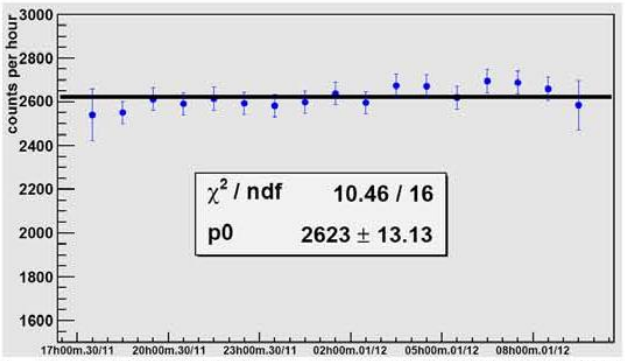

Fig. 41: *Rate detected with the LND 253109 counter 30.11.2010-01.12.2010 in channels 170-940 of the spectrum shown on the Fig. 40.*

For rough comparison of results of measurements with 2 detectors we compared counting rate detected with each detector inside of PE tube to the mass of He-3 in the detectors. Results presented in the table 7.

Table 7: Comparison of results of neutron flux measurements with CHM-57 and LND 253109 detectors.

Detector	He-3 mass, mg	Counts / h / 1 g He-3
CHM-57	316	2434
LND 253109	1304	2012

As clear from the tale 7 the received results are very similar. It has to be noted that results can not be same without detailed MC. Received agreement means that neutrons are measured in right way on both detectors, but LND 253109 one requires QDC or longer time shaping amplifier in the electronics' chain.

Personal involved in this activity from JINR side: S. Rozov, S. Semikh and E. Yakushev.